Investigating the Geminal Diamine Intermediate of *Yersinia pestis* Arginine Decarboxylase with Substrate, Product, and Inhibitors Using Single Wavelength Stopped-Flow Spectroscopy†

Korie G. Counts,‡ Isaac Wong,§ and Marcos A. Oliveira*,‡

Departments of Pharmaceutical Sciences, Feik School of Pharmacy, University of the Incarnate Word, San Antonio, Texas 78209, and Department of Pharmaceutical Sciences, College of Pharmacy, Markey Cancer Center and Department of Biochemistry, University of Kentucky, Lexington, Kentucky

Received June 23, 2006; Revised Manuscript Received October 16, 2006

ABSTRACT: The reaction mechanism of *Yersinia pestis* arginine decarboxylase has been investigated using a series of substrate, product, and inhibitors. Using single wavelength stopped-flow spectroscopy, novel mechanistic features were noted in the presence of the product, agmatine. By focusing on the excitation and emission wavelengths of the geminal diamine intermediate, we were able to monitor the formation and decay of two different geminal diamine species. Experiments revealed that the enzyme exists in two different conformational states—one that binds ligand and one that does not. The on and off rates for the conversion between the two conformational states was determined to be 390 s^{-1} and 880 s^{-1}, respectively. The K_D for agmatine binding was 6 mM. In addition, experiments revealed a pH-dependent conversion between two states of the enzyme. The deprotonated form of the enzyme binds ligand more slowly than the protonated form. The rates for the formation of the geminal diamine and external aldimine in this pathway were determined to be 25 and 4 s^{-1}, respectively. There is also a slow interconversion between the protonated and deprotonated enzymes that has a pK_a of ∼8.0. Finally, the formation of the geminal diamine was determined to be Mg^{2+}-dependent.

Yersinia pestis, the etiological agent responsible for causing bubonic and pneumonic plague, is classified as a category A biological agent. According to the CDC,[1] category A agents meet the following criteria: (i) must be easily transmitted from person to person, (ii) result in high mortality and have a major impact on public health, (iii) can cause public panic and social disruption, (iv) require special action for public preparedness, and (v) have the potential for delivery in a weapon (*1*). In order to combat potential antibiotic resistance occurring as a result of natural mutations or by purposeful genetic manipulation, novel antimicrobial agents need to be developed against *Y. pestis*.

Y. pestis is known to require biofilm for transmission of the bacteria from rodents to humans (*2*, *3*). It has been shown that polyamines are essential for mature biofilm formation in *Y. pestis* (*4*). In bacteria, there are two pathways available for polyamine biosynthesis, ornithine decarboxylase (ODC), and arginine decarboxylase (ADC). Evidence suggests that ADC is the primary polyamine biosynthetic enzyme in *Y. pestis* (*4*). ADC, which catalyzes the decarboxylation of L-arginine to form agmatine, is a fold III, pyridoxal-5′-phosphate (PLP)-dependent enzyme. It is a unique enzyme because, in addition to PLP, it also requires Mg^{2+} for activity. Because of its role in biofilm formation and the novel requirement of Mg^{2+}, ADC becomes an attractive target for drug design.

PLP-dependent enzymes are capable of catalyzing many different types of reactions, including decarboxylation, transamination, racemization, retro aldol cleavage, and β-elimination (*5*). In the case of PLP-dependent decarboxylases, there are common mechanistic features (Scheme 1). First, there is an imine bond between the cofactor and the ϵ-amino group of an active site lysine residue known as an internal aldimine. Upon substrate binding, the ϵ-amino group of lysine is displaced by the amino group on the substrate, forming an intermediate called an external aldimine. Substrate is then decarboxylated, forming a quinonoid intermediate. This intermediate is then protonated at C_α, generating an external aldimine. This is then followed by product release and the regeneration of the cofactor−lysine imine bond.

When the amino acid substrate binds to the cofactor to displace the ϵ-amino group of the active site lysine, a transient intermediate is formed, known as a geminal diamine. The first spectroscopic evidence for the existence of this intermediate in the context of an enzyme was seen in

† This work was supported by an NIH Southeast Regional Center for Excellence in Biodefense (SERCEB) developmental grant (UF4 AI057175) to M.A.O. K.G.C. was supported by the Graduate School Allocated fellowship and Kentucky Opportunity fellowship from the University of Kentucky and the American Foundation for Pharmaceutical Education (AFPE) Pre-Doctoral fellowship.

* Corresponding author. Phone: (210) 805-3012. Fax: (210) 805-3013. E-mail: oliveira@uiwtx.edu.

‡ Department of Pharmaceutical Sciences, College of Pharmacy.

§ Markey Cancer Center and Department of Biochemistry.

[1] Abbreviations: ADC, arginine decarboxylase; ODC, ornithine decarboxylase; PLP, pyridoxal-5′-phosphate; CDC, Center for Disease Control; SHMT, serine hydroxymethyltransferase; ACC, 1-aminocyclopropane-1-carboxylate; HisC, histidinol phosphate aminotransferase; IPTG, isopropyl-β-D-thiogalatopyranoside; TIM, triose phosphate isomerase.

10.1021/bi061260h CCC: $37.00
Published on Web 12/14/2006

Scheme 1: General Mechanism for PLP-Dependent Decarboxylases

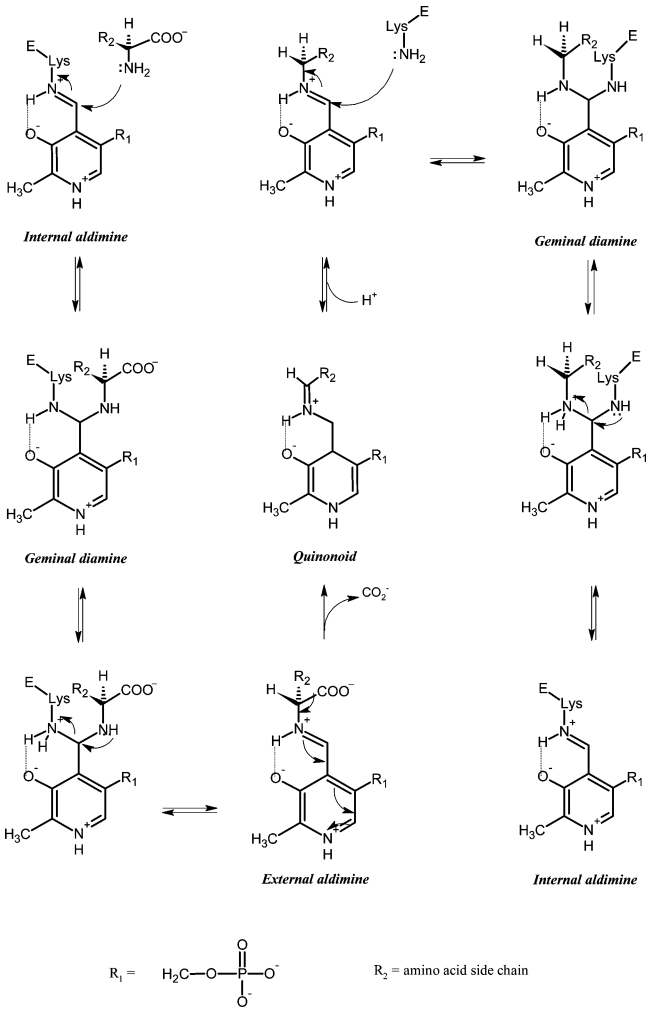

a transient kinetic study of serine hydroxymethyl transferase (SHMT) (*6*). In this study, they observed a fluorescence emission at 395 nm upon excitation at 343 nm. The lack of a fluorescence emission for native SHMT at 395 nm upon excitation at 343 nm permitted Schirch to monitor fluorescence emission changes at ~395 nm. The evidence presented by Schirch shows a complex formed in a bimolecular step representing the first covalently bound species. Based upon this observation, the geminal diamine was the only intermediate that could be assigned as the 343 nm absorbing complex. Another example in which the geminal diamine intermediate was assigned used rapid scanning and single-wavelength stopped-flow spectroscopy was in the context of tryptophan synthase, where it was proposed that a species with a $\lambda_{max} \leq 340$ nm was the geminal diamine intermediate (*7*).

There are other spectroscopic investigations that show the difficulty in making a direct correlation between the geminal diamine intermediate and fluorescence emission at ~400 nm with excitation at 330 nm. This occurs because the enolimine form of the Schiff base can display a similar fluorescence emission, depending on the environment of the intermediate. Florescence emission has been observed in *F. lutescens* L-lysine-α-ketoglutarate ϵ-aminotransferase (*8*), *E. coli* glutamate decarboxylase (*9*), and *Treponema denticola* Cystalyn (*10*). However, solution studies with model PLP derivatives clearly show that spectral properties depend on the nature of the environment (*11*−*14*). In the case of ADC, we see no fluorescence emission of the native enzyme at ~400 nm upon excitation at 330 nm (*15*). This evidence supports using fluorescence for the detection of the geminal diamine intermediate, as was used in SHMT.

Recently, structural evidence for the existence of the geminal diamine has been shown. A group working with rabbit cytosolic SHMT was able to model the geminal diamine intermediate using the structure of a reduced form of the internal aldimine, along with known constraints on substrate binding. They were also able to accumulate the geminal diamine complex by mutating Thr226 to Ala. Because Thr226 is responsible for hydrogen bonding to the ϵ-amino group of Lys229, thereby favoring the formation of the external aldimine intermediate, mutating this residue to Ala causes the removal of Lys229 from the cofactor to become much slower and the geminal diamine intermediate to accumulate (*16*). Later, another group crystallized murine cytoplasmic SHMT in complex with the geminal diamine (*17*). There also exists structural evidence for the geminal diamine intermediate in *E. coli* histidinol phosphate aminotransferase (HisC) (*18*) in *Pseudomonas* 1-aminocyclopropane-1-carboxylate (ACC) deiminase (*19*) and also for mammalian ornithine decarboxylase (*20*).

In this paper, an investigation into the mechanistic details of *Yersinia pestis* arginine decarboxylase was performed using single-wavelength-stopped flow spectroscopy. By focusing on the known characteristic absorbance and fluorescence wavelengths of the geminal diamine species (Scheme 2), it was possible to monitor the formation of the geminal diamine intermediate.

MATERIALS

Materials. Imidazole, $MgCl_2 \cdot 6H_2O$, agmatine sulfate salt, L-arginine·HCl, L-argininamide·2HCl, L-arginine methyl ester·2HCl, pyridoxal-5′-phosphate (PLP), MES, and HEPES were all purchased from Sigma. Ni−NTA agarose was purchased from Qiagen. Tris was obtained from Invitrogen. Centricon concentrators were purchased from Fisher. Phast gel materials were purchased from Amersham.

Protein Purification. Transformed *E. coli* cells expressing the *Y. pestis* ADC gene (*speA*) were grown to an $OD_{600} > 0.6$ at 37 °C and then induced with a final concentration of 1 mM IPTG. The cells were then allowed to grow at 25 °C overnight and were harvested by centrifugation. The cell pellet was resuspended in buffer B (20 mM Tris pH 8.5, 10 mM $MgCl_2$, 1 mM PLP). The resuspended cells were disrupted by sonication and clarified by centrifugation (8000 rpm in a Beckman Type 45-Ti rotor for 20 min). The clarified supernatant was then applied to a Ni−NTA agarose column. Following the application of the supernatant, the column was washed with 125 mL of buffer B. This wash was followed with 125 mL of buffer B containing 30 mM imidazole. The protein was eluted in 125 mL of buffer B containing 90 mM imidazole. The protein collected was exchanged into the appropriate buffer by ultracentrifugation using a Centricon30 device. Protein concentration was determined by measuring the absorbance at 280 nm. Protein purity was determined using the Phast gel system.

Pre-Steady-State Kinetics of Substrate, Product, and Inhibitor with ADC by Single-Wavelength Stopped-Flow

Scheme 2: Spectroscopic Properties of PLP Complexes Focused on in This Work[a,b]

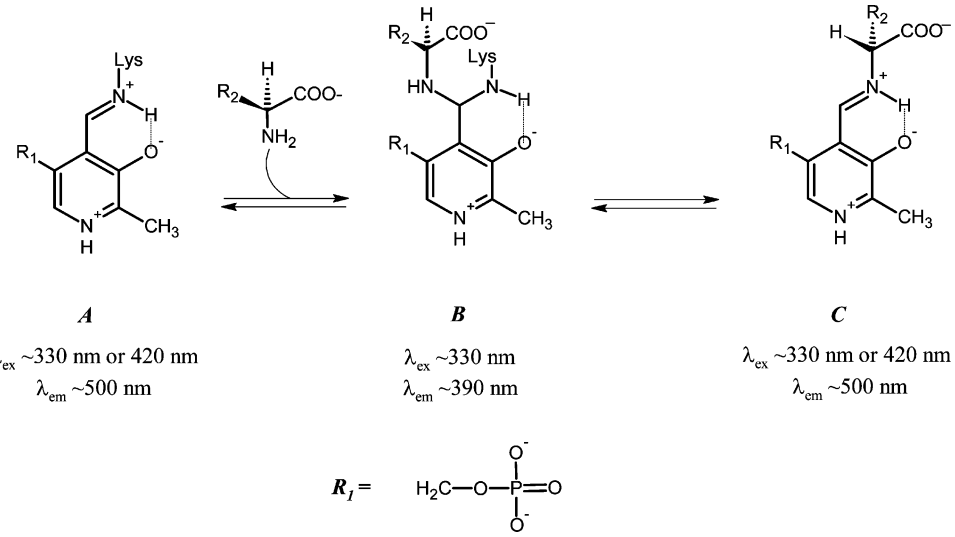

[a] (A) Internal aldimine, (B) geminal diamine, and (C) external aldimine. [b] R_2 represents the amino acid side chain.

Scheme 3: Substrate, Product, and Inhibitors Used in This Work[a]

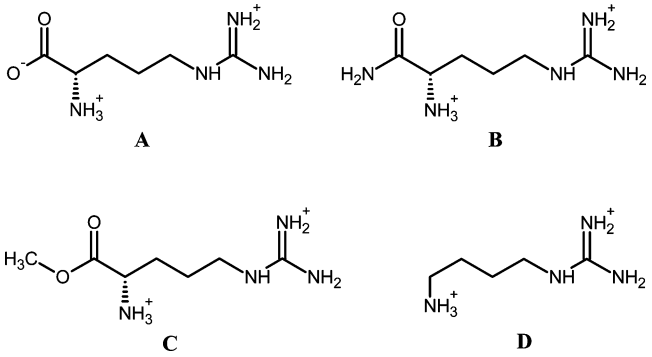

[a] (A) L-Arginine, (B) L-argininamide, (C) L-arginine methyl ester, (D) agmatine.

Spectroscopy. The pre-steady-state kinetics of ADC reacting with substrate, product, and inhibitors (see Scheme 3 for structures) were monitored at 4 °C using a Kintek SF2001 pneumatically driven stopped-flow instrument with an upgraded 150 W xenon arc lamp mounted vertically in a Hamamatsu lamp housing a Hamamatsu monochromator. Traces were collected by exciting at 330 nm and monitoring fluorescence at 400 nm to observe geminal diamine species. The final concentration of ADC was 0.1 mM in 0.1 M HEPES, 5 mM $MgCl_2$, pH 7.5. A final concentration of 50 mM was used for substrate, product, and inhibitors.

Agmatine Concentration Series. ADC (0.2 mM) and agmatine solutions were prepared in kinetics buffer (0.1 M HEPES, 5 mM $MgCl_2$, pH 7.5). Traces were taken at 4 °C for agmatine concentrations between 50 and 5 mM. Data was collected for $\lambda_{ex} = 330$ nm ($\lambda_{em} = 400$ nm) and $\lambda_{ex} = 420$ nm ($\lambda_{em} > 490$ nm). The following equation was used to fit the data collected at $\lambda_{ex} = 330$ nm ($\lambda_{em} = 400$ nm):

$$y = \sum_{i=1}^{n} A_i(1 - e^{-k_i t}) + C \qquad (1)$$

where n is the number of phases, A_i and k_i are the amplitude and the apparent rate constant, k_{obs}, for the i^{th} phase, respectively, and C is a constant. Because the number of fitted parameters became unmanageable as n increased beyond 3, most time courses were fitted in two separate time segments corresponding to the 3 and 100 ms transients, constraining some amplitudes and rate constants in order to obtain a more robust fit on the rest.

The k_{obs} values for the fast 3 ms transient of agmatine binding were plotted versus agmatine concentration and fitted to the following equation:

$$y = k_1 + \frac{K_D k_{-1}}{[L] + K_D} \qquad (2)$$

for rapid equilibrium binding of ligand to two slowly interconverting pre-existing forms of enzyme.

pH Titrations. ADC (0.2 mM) and agmatine solutions were prepared in a MES/Tris buffer. The pH of the solution was controlled by varying the ratio of MES and Tris. Traces were collected at 4 °C for agmatine concentrations between 50 and 5 mM at the following pH values: 7.12, 7.46, 7.93, 8.43, and 9.04.

To investigate the relationship between the two phases with changing pH, the area under each portion of the traces was determined. Phase 1 was considered from 0.001 to 0.03 s. Phase 2 was considered from 0.031 to 1.01 s. The area under each of these sections was determined using Kaleidagraph 4.0. Each area was then divided by the area under phase 1 (the smaller area). The ratio of the area under phase 2 to the area under phase 1 was plotted versus pH in Kaleidagraph. The resulting curve was fit using the following equation:

$$y = \frac{y_{min} + (y_{max} - y_{min})}{1 + (pH/pK_a)^n} \qquad (3)$$

Mg^{2+} Dependence Experiments. ADC (0.2 mM) was washed with EDTA to remove Mg^{2+}. The enzyme was then exchanged into 0.1 M HEPES, pH 7.5. Agmatine (100 mM) was prepared in 0.1 M HEPES, pH 7.5. Traces were collected at 4 °C using $\lambda_{ex} = 330$ nm ($\lambda_{em} = 400$ nm) and $\lambda_{ex} = 420$ nm ($\lambda_{em} > 490$ nm).

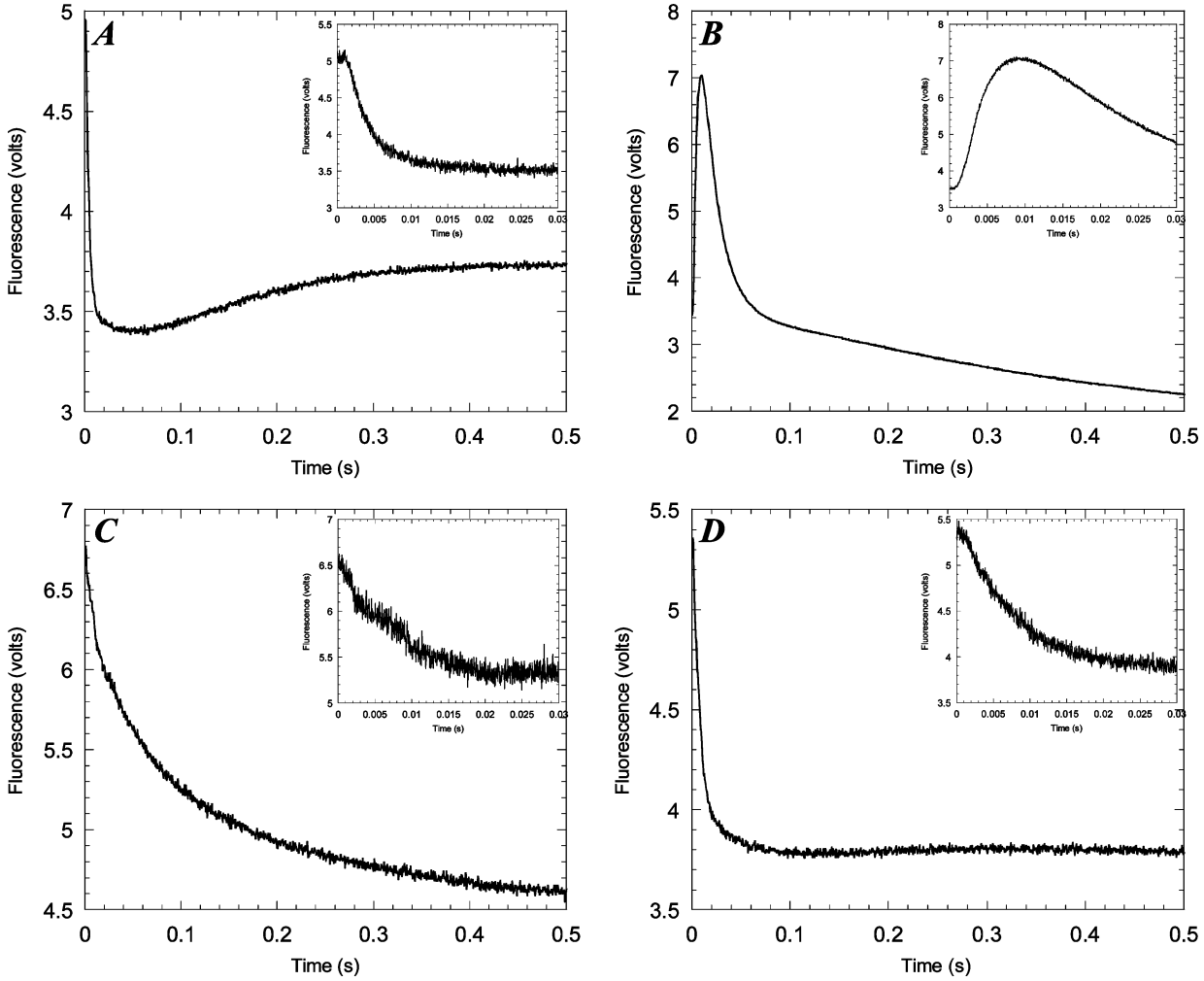

FIGURE 1: Stopped-flow fluorescence traces of ADC with L-arginine (A), agmatine (B), L-argininamide (C), and L-arginine methyl ester (D). All traces were collected using 0.1 mM ADC and 50 mM substrate, product, or inhibitor. Spectra were collected monitoring $\lambda_{ex} = 330$ nm and $\lambda_{em} = 400$ nm. Insets show 0−30 ms time scale.

RESULTS

Pre-Steady-State Kinetic Analysis of ADC in the Presence of Substrate, Product, and Inhibitors. Single-wavelength stopped-flow spectroscopy was used to investigate the binding of substrate, product, and inhibitors to ADC (Scheme 3). This method can be used to probe for specific intermediates in the PLP-dependent reaction mechanism by exciting with and monitoring at optimal wavelengths corresponding to the excitation and emission maxima. Fluorescence spectra were collected at 4 °C so that all relevant intermediates were observable and not completed in the dead time of the instrument. The compounds used in these experiments were L-arginine (substrate), agmatine (product), L-arginine methyl ester, and L-argininamide (inhibitors). The inhibitors were chosen because of their inability to undergo decarboxylation, the mechanistic step following external aldimine formation. Results are shown in Figure 1.

Analysis of ADC Pre-Steady-State Kinetics with Agmatine. The results of the pre-steady-state kinetic experiments with ADC in the presence of agmatine are shown in Figure 2. The traces shown were collected at $\lambda_{ex} = 330$ nm and $\lambda_{em} = 400$ nm to isolate the geminal diamine species. Under the experimental conditions shown in this figure, two transients were apparent at all concentrations of agmatine, one peaking in the 3 ms time range and the other peaking around 100 ms. Additionally, at decreasing agmatine concentrations, three changes in the geminal diamine fluorescence traces

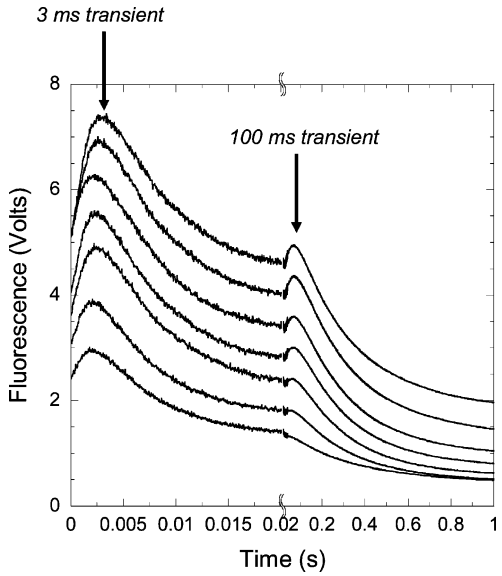

FIGURE 2: Single-wavelength stopped-flow fluorescence traces at decreasing agmatine concentrations. Traces were collected at $\lambda_{ex} = 330$ nm and $\lambda_{em} = 400$ nm with 0.1 mM ADC and agmatine concentrations between 50 and 5 mM.

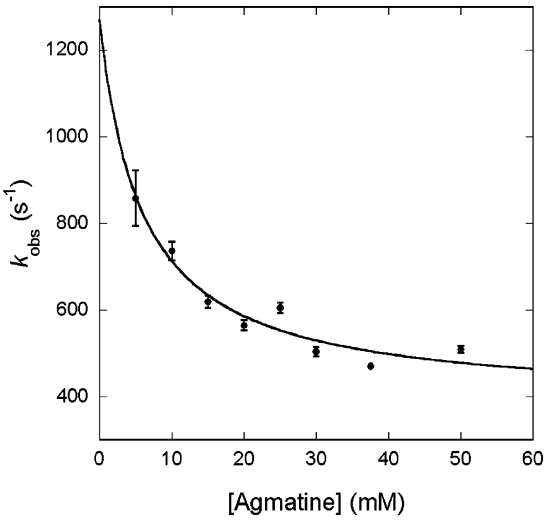

FIGURE 3: Determination of individual rate constants for Scheme 4. Plot represents the k_{obs} values determined from λ_{ex} = 330 nm and λ_{em} = 400 nm data for 50−5 mM agmatine.

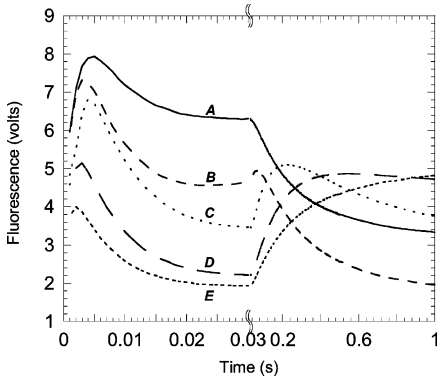

FIGURE 4: pH dependence of geminal diamine fluorescence traces. Traces were collected at λ_{ex} = 330 nm and λ_{em} = 400 nm using 0.1 mM ADC and 50 mM agmatine at pH 7.12 (A), pH 7.46 (B), pH 7.93 (C), pH 8.46 (D), and pH 9.04 (E).

became apparent: (1) a decrease in amplitude in the fast transient at ~3 ms, (2) a decrease in amplitude in the slow transient at ~100 ms, and (3) a shift of the fast transient peak to the left toward earlier time points, suggesting an increase in the rate of its formation.

Each of these time courses were fitted in two time segments that separately delineated each transient. The best-fit values of the apparent rate constant, k_{obs}, for the formation of the 3 ms transient are shown in Figure 3 as a function of agmatine concentration. The rate constant for the decay of the 3 ms transient was 180 s^{-1} and was agmatine concentration-independent. Additional slower phases corresponding to the 100 ms transient were fitted separately and yielded concentration-independent rate constants of 25 and 4 s^{-1}.

Analysis of pH-Dependent Geminal Diamine Fluorescence Spectra. Figure 4 shows the pH-dependent fluorescence traces for the geminal diamine intermediate collected at λ_{ex} = 330 nm and λ_{em} = 400 nm. With each increase in pH, the 3 ms transient decreases in amplitude; conversely, the amplitude of the 100 ms transient increases with each increase in pH accompanied by an amplitude stabilization at pH 9.04 after 1 s. To investigate the relationship between these two transients, the area under each curve was determined. The relationship between the transients is shown in Figure 5.

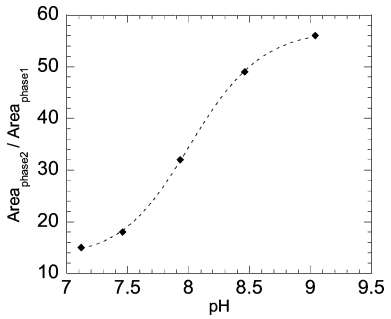

FIGURE 5: Relationship between the area under transient 1 and 2 of the curves in Figure 4 with increasing pH.

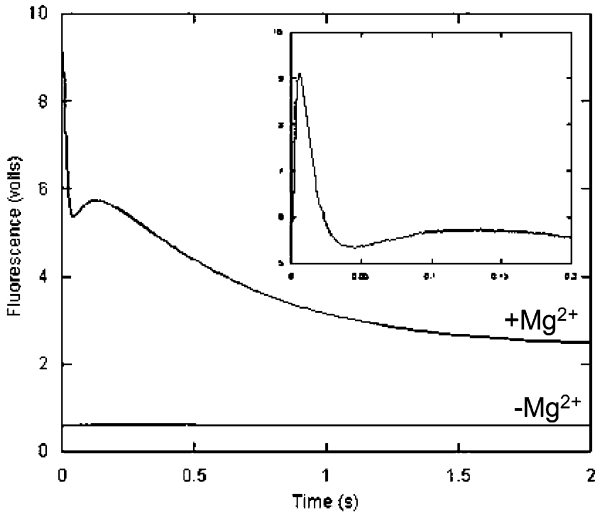

FIGURE 6: Dependence of geminal diamine formation on the presence of Mg^{2+}. Data was collected at λ_{ex} = 330 nm and λ_{em} = 400 nm. The inset shows the details of transient 1 in the geminal diamine trace. Experimental conditions included 0.1 mM ADC ± Mg^{2+} and 50 mM agmatine in 0.1 M HEPES, pH 7.5.

Analysis of Mg^{2+} Dependence Experiments. Figure 6 shows the geminal diamine traces in the presence and absence of Mg^{2+}. ADC + Mg^{2+} produces a trace like that seen in the other experiments discussed. However, in ADC− Mg^{2+}, only a baseline trace is collected.

DISCUSSION

The chemistry of PLP-catalyzed reactions is generally well understood as outlined in Scheme 1. However, the overall mechanisms of PLP-dependent enzymes extend beyond the flow of electrons at the cofactor and are separately constrained by the structural−functional characteristic of each individual protein (*5*, *21*). Thus, whether the common aldimine adduct between PLP and the amino acid is fated for transamination, decarboxylation, or cleavage of the C_α−C_β bond is ultimately dictated by the conformation of the polypeptide chains forming the active site of each enzyme. To truly understand the reaction mechanism of decarboxylation by an enzyme like ADC, therefore, requires understanding the structure−function relations and conformational constraints of the active site that steer and position the PLP−substrate adduct for the exclusive regio- and stereospecific cleavage of the C_α−carboxylate bond.

In this report, initial stopped-flow fluorometry observations of the rapid kinetics of substrate binding by the ADC from *Y. pestis* reveal the presence of numerous novel conforma-

Scheme 4: Model of the Mechanism of Agmatine Binding by ADC[a]

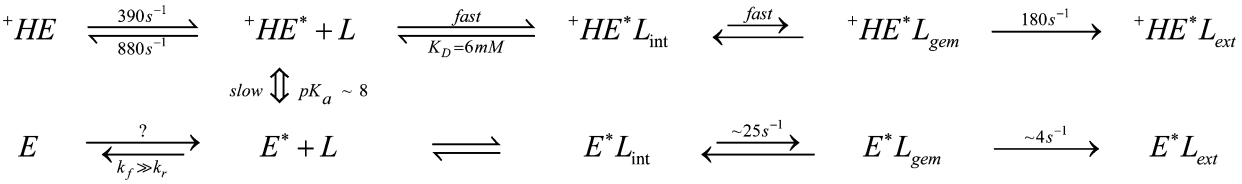

[a] Top path represents the enzyme in the protonated form and gives rise to the 3 ms transient formation of the geminal diamine. The bottom path represents the enzyme in the deprotonated form and gives rise to the 100 ms transient. The rate of interconversion between the two paths must be at least slower than the ~25 s^{-1} rate constant for forming the 100ms transient and is likely to be slower than the 4 s^{-1} rate constant for its decay. HE* and E* represent the forms of the enzymes competent to bind agmatine (L). The subscripts int, ext, and gem refer to the internal aldimine, the external aldimine, and the geminal diamine species, respectively.

tional states of the enzyme involved in the binding and formation of the aldimine adduct with the PLP. These methods identify reaction intermediates that appear on much shorter time scales than steady-state kinetics can reveal and allows one to focus in on the transient intermediate states during a single steady-state turnover.

Single-Wavelength Stopped-Flow Fluorometry. A multiwavelength stopped-flow approach has been used previously to elucidate the reaction mechanism of the related enzyme, ODC (*22*). The approach in this report differs in exploiting the unique and characteristic fluorescence properties of the various PLP intermediates in order to maximize the signal for detecting changes in concentrations of a particular species, namely, the geminal diamine intermediate. In the multiwavelength approach, data is collected across the entire wavelength spectrum and deconvoluted in order to deduce a set of basis spectra that in turn defines intermediates. The strength of this approach lies in its ability to model all intermediates simultaneously; however, in so doing, the signal-to-noise ratio of the data set is inevitably compromised. This is because, by scanning across the entire wavelength spectra, data is collected at wavelengths without regards to whether that wavelength is unique or common to each intermediate. In the extreme case, at isosbestic points, the collected data contributes no signal for changes in intermediate concentrations and therefore only contributes noise to the data set. In contrast, by focusing on a single intermediate, the geminal diamine, all data was collected in this study at the characteristic fluorescence emission peak of the intermediate (λ_{ex} = 330 nm, λ_{em} = 390 nm), thereby maximizing the signal. This was critical for the success in observing this rapidly formed and degenerated transient due to the inherent dead time of the stopped-flow technique.

Spectroscopic studies of PLP derivatives in solution and in the context of an enzyme show that the different species, in particular the ketoenamine and enolimine, have spectral properties that are highly dependent upon the environment. Therefore, even though there are reports of enolimine forms of PLP displaying fluorescence at ~400 nm with excitation at 330 nm, there are also reports showing lack of fluorescence at this wavelength. In the case of ADC, we have investigated the fluorescence of the enolimine and ketoenamine forms of holoenzyme, as well the external aldimine forms of ADC in the presence of different ligands. Our investigation has been reported in Balbo et al. (*15*). Using UV−vis spectroscopic measurements, we were able to observe the interconversion between ketoenamine and enolimine forms of holoenzyme and external aldimine forms of the enzyme with a variety of adducts. In all cases, the predominant form observed is the ketoenamine form. However, we also saw the interconversion of one form with changes in pH. In the same study, we did not observe fluorescence at ~400 nm with excitation at 330 nm in either holoenzyme or any of the external aldimine forms investigated. We concluded that, in the case of ADC, PLP is observed predominantly in the ketoenamine form. In SHMT, a species absorbing at 343 nm with no significant fluorescence at ~400 nm in the native enzyme was identified as the geminal diamine intermediate. This initial observation led us to investigate fluorescence at <400 nm with excitation at 330 nm to determine whether or not we were able to observe the rapidly forming geminal diamine intermediate.

Initially, data was collected in the presence of substrate (L-arginine), product (agmatine), and inhibitors (L-argininamide and L-arginine methyl ester). From these experiments, it was noted that in the presence of agmatine it was possible to monitor the formation and decay of a geminal diamine species at ~3 ms. This was not observable in the L-arginine, L-argininamide, or L-arginine methyl ester traces because the formation of the geminal diamine intermediate is generally too fast to be observed. Its presence is inferred from the observable loss of fluorescence upon its conversion to the external aldimine.

Because examining ADC in the presence of agmatine made it possible to monitor the geminal diamine and the aldimine species, experiments were performed that specifically targeted the interaction between ADC and agmatine. The data collected was fit to a function of multiple exponential phases (eq with each exponential phase defined by an amplitude and an apparent rate constant (k_{obs})). Elementary rate constants (k_1, k_{-1}, etc.) can be extracted by fitting the ligand concentration-dependence of k_{obs}. The fits obtained for ADC in the presence of agmatine revealed a unique mechanism containing at least five exponential phases including the formation and decay of two different geminal diamine species (see Figure 2), a reactive intermediate that is usually formed too rapidly to be observed directly.

Concentration Dependency of Agmatine Binding Reveals Two Conformations of ADC. A uniquely salient feature of the concentration series was the observation that the 3 ms transient occurred at increasingly earlier times as the concentration of agmatine was lowered, indicating that the rate constant for geminal diamine formation appeared faster at lower concentrations of ligand. Mechanistically, this seemingly counterintuitive observation requires that the enzyme pre-exists in two states (Scheme 4), only one of which is capable of binding the ligand, as illustrated in the following reaction:

$$E \underset{k_{-1}}{\overset{k_1}{\rightleftharpoons}} E' + L \underset{k_{-2}}{\overset{k_2[L]}{\rightleftharpoons}} E'L$$

Solving the system of differential equations for Scheme 4 using the matrix method (*23*, *24*) yields eigenvalues, $\lambda_{\pm}$, as shown below:

$$\lambda_{\pm} = k_1 + k_{-1} + k_2[L] + k_{-2} \pm \frac{\sqrt{(k_1 + k_{-1} + k_2[L] + k_{-2})^2 - 4(k_1k_2[L] + k_1k_{-2} + k_{-1}k_{-2})}}{2} \quad (4)$$

These eigenvalues correspond directly to the observed rate constants for the fast and the slow phases, respectively. Equation 4 can be further simplified using the square-root approximation (*23*, *24*) to yield the observed rate constants shown below:

$$k_{obs,fast} = \lambda_+ = k_1 + k_{-1} + k_2[L] + k_{-2}$$
$$k_{obs,slow} = \lambda_- = \frac{k_1k_2[L] + k_1k_{-2} + k_{-1}k_{-2}}{k_1 + k_{-1} + k_2[L] + k_{-2}} \quad (5)$$

If the binding of the ligand occurs via a rapid-equilibrium step, i.e., $k_2[L]$ and $k_{-2} \gg k_1$, k_{-1}, the fast exponential phase corresponding to the initial binding of L by E′ becomes too fast to be seen. The observable transient, therefore, actually reflects additional binding that is rate-limited by the slower conversion of E to E′. This allows the expression for $k_{obs,slow}$ given by eq 5 to be further simplified:

$$k_{obs} = \frac{k_1k_2[L] + k_1k_{-2} + k_{-1}k_{-2}}{k_2[L] + k_1 + k_{-1} + k_{-2}}$$
$$\approx \frac{k_1k_2[L] + k_1k_{-2} + k_{-1}k_{-2}}{k_2[L] + k_{-2}} \qquad k_2[L] + k_{-2} \gg k_1 + k_{-1}$$
$$= \frac{k_1[L] + \frac{k_{-2}}{k_2}k_1 + \frac{k_{-2}}{k_2}k_{-1}}{[L] + \frac{k_{-2}}{k_2}}$$
$$= \frac{k_1[L] + K_Dk_1 + K_Dk_{-1}}{[L] + K_D}$$
$$= k_1 + \frac{K_Dk_{-1}}{[L] + K_D} \quad (6)$$

The inverted concentration dependency of k_{obs} is readily apparent by noting that the limits at [L] = 0 and [L] → ∞ are $k_1 + k_{-1}$ and k_1, respectively. The fit of the data (Figure 3) yielded values for k_1 and k_{-1} of 390 and 880 s^{-1}, respectively, and a K_D for initial agmatine binding of 6 mM. Experimental limits to detecting transients that come and go in less than 3 ms precluded the collection of more data points at lower concentrations of agmatine for the purpose of improving the estimate on k_{-1}, which is largely dependent on the extrapolated *y*-intercept value. However, k_1 was well-defined by the asypmtotic limit at higher agmatine concentrations.

The ratio of k_1 to k_{-1} defined an equilibrium constant of 2.25 in favor of the form of the enzyme that did not bind agmatine. In addition, the formation of the initial geminal diamine species observed with agmatine was rate-limited by the conversion of enzyme to a form capable of binding the agmatine. Furthermore, this slower rate was unique to the reaction product agmatine; i.e., L-arginine and other substrate analogues all showed much faster rates of geminal diamine formation, suggesting that E and E′ may represent forms of the enzyme for binding substrate and releasing product, respectively. This difference may reflect the loss of the stereocenter at C_α, although more direct lines of evidence both structurally and functionally will be needed to verify this.

pH Profile Reveals Two Protonation States of ADC. In addition to the two conformational states of ADC revealed by the concentration dependencies, the presence of two distinct transients, one at 3 ms and the other at 100 ms, further reveals the existence of two distinct geminal diamine species. If two convergent paths were to lead to a common fluorescent intermediate, the second transient would not be detected. This is because the rate of decay for the common geminal diamine intermediate is faster than the rate of appearance of the second transient. Thus, any geminal diamine formed via the slower path would not accumulate. The observation of two separate transients, therefore, dictates that two distinct geminal diamine species be present on divergent or parallel paths.

The pH dependencies of the two transients (Figure 4) support this and further suggest that the two pathways differ in the protonation state of the enzyme. Using this observation and the previously described experimental results, a minimal mechanism was developed (Scheme 4). In this mechanism, ADC exists in two different protonation states, both capable of forming the geminal diamine intermediate. However, the protonated form more rapidly reaches that intermediate, resulting in the very fast formation of the first phase (Figure 2).

One possibility for the slower transition to the geminal diamine in the deprotonated form of the enzyme is interference with a hydrogen bond network that regulates the PLP cofactor. Another possibility for the difference in the enzyme species is the protonation of an amino acid residue that is critical to geminal diamine formation. A candidate for this amino acid is an active site cysteine residue (Figures 5 and 7) based on the apparent pK_a. In *T. brucei* ODC, structural evidence shows that this cysteine residue (C360; C529 in ADC) rotates close enough to the C_α carbon to protonate the intermediate formed after decarboxylation has occurred (*25*). By comparing the areas under the two phases in the pH titration curves (Figure 5), it was discovered that their relationship fit to a sigmoidal curve. This curve fit revealed a pK_a value of 8.0, which is approximately the pK_a of the side-chain proton on a cysteine residue. In the protonated form, the cysteine residue may be rotated out of the active site, as seen in *T. brucei* ODC (*25*). In this situation, the residue would most likely be hydrogen bonded to another residue until after substrate binding and decarboxylation occurred. The cysteine would then rotate near the C_α carbon and donate the side chain proton, allowing catalysis to proceed. If the cysteine side chain were deprotonated, it would lose the stabilizing hydrogen bond and as a result

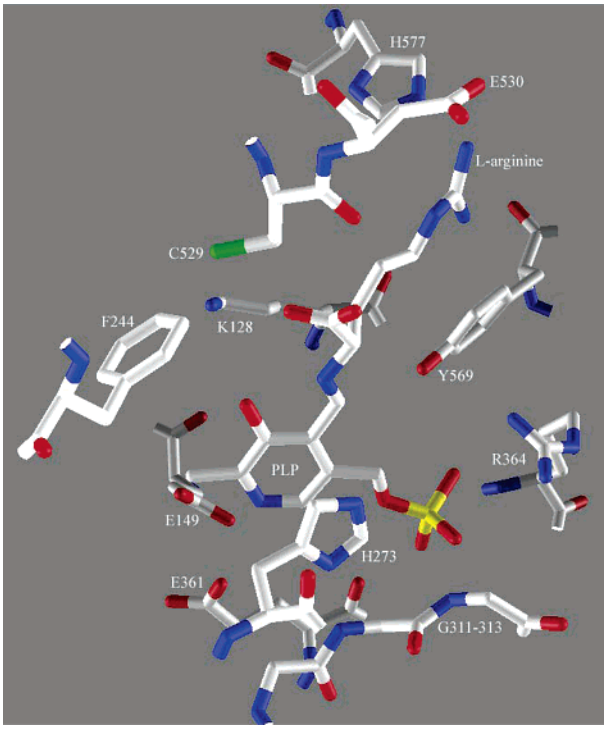

FIGURE 7: Model of ADC active site with bound substrate, L-arginine. Important active site residues are labeled.

could interfere with proper substrate binding. This would slow the transition from the internal aldimine to the geminal diamine. The later-forming geminal diamine species would become more prominent with an increase in pH, which is what is observed in Figure 4.

Attempts to fit all of the data globally to a unique kinetic mechanism by simulation were complicated by the presence of the two protonation states. In addition to the large number of parameters needed for such a simultaneous fit, the two parallel reaction pathways would additionally necessitate the assignment of each exponential phase to the path corresponding to the appropriate protonation state. Within a concentration series alone at a single pH, this was impossible as all exponential phases with the exception of the first followed a similar concentration dependency of decreasing amplitude and identical rate constants with decreasing concentration. A more detailed analysis of the combination of pH and concentration data beyond the scope of the present report would be needed to deconvolute the slower multitude of exponential phases of agmatine binding.

Geminal Diamine Formation Depends on Mg^{2+}. In addition to noting a pH dependency, we also showed that the formation of the geminal diamine species was dependent upon the presence of Mg^{2+} (Figure 6). We generated an apo form of ADC that lacks Mg^{2+} and retains PLP. This form of the enzyme does not interfere with the oligomeric state of ADC based on light scattering experiments (*26*). Our results suggest that Mg^{2+} is essential in the formation of the geminal diamine species. ADC contains a TIM barrel domain for PLP binding, a domain that is well-known for binding magnesium. This is the case of the enolase superfamily (*27*). We considered the possibility that, like the enolase superfamily, we would find a cluster of acidic residues mapping to the C-terminal end of the TIM barrel. The model of ADC, however, does not reveal such a cluster (Figure 7). It is noteworthy that the ~100 residue insertion of unknown structure that maps to the interface between the TIM barrel and the mostly C-terminal β-sandwich domain does have a high content of acidic residues (17 residues out of 100). This suggests that this insertion may bind Mg^{2+} and regulate the chemical events at the TIM barrel domain. Whatever the scenario, our data suggests an unprecedented and novel mode of regulation of PLP chemistry by ADC.

REFERENCES

1. Bhalla, D. K., and Warheit, D. B. (2004) *Toxicol. Appl. Pharmacol. 199*, 71−84.
2. Hinnebusch, B. J., Perry, R. D., and Schwan, T. G. (1996) *Science 273*, 367−370.
3. Kirillina, O., Fetherston, J. D., Bobrov, A. G., Abney, J., and Perry, R. D. (2004) *Mol. Microbiol. 54*, 75−88.
4. Patel, C. N., Wortham, B. W., Lines, J. L., Fetherston, J. D., Perry, R. D., and Oliveira, M. A. (2006) *J. Bacteriol. 188*, 2355−2363.
5. Toney, M. D. (2005) *Arch. Biochem. Biophys. 433*, 279−287.
6. Schirch, L. (1975) *J. Biol. Chem. 250*, 1939−1945.
7. Roy, M., Miles, E. W., Phillips, R. S., and Dunn, M. F. (1988) *Biochemistry 27*, 8661−8669.
8. Misono, H., and Soda, K. (1977) *J. Biochem. (Tokyo) 82*, 535−543.
9. Shukuya, R., and Schwert, G. W. (1960) *J. Biol. Chem. 235*, 1653−1657.
10. Bertoldi, M., Cellini, B., Clausen, T., and Voltattorni, C. B. (2002) *Biochemistry 41*, 9153−9164.
11. Johnson, G. F., Tu, J. I., Bartlett, M. L., and Graves, D. J. (1970) *J. Biol. Chem. 245*, 5560−5568.
12. Cortijo, M., Steinberg, I. Z., and Shaltiel, S. (1971) *J. Biol. Chem. 246*, 933−938.
13. Shaltiel, S., and Cortijo, M. (1970) *Biochem. Biophys. Res. Commun. 41*, 594−600.
14. Bridges, J. W., Davies, D. S., and Williams, R. T. (1966) *Biochem. J. 98*, 451−468.
15. Balbo, P. B., Patel, C. N., Sell, K. G., Adcock, R. S., Neelakantan, S., Crooks, P. A., and Oliveira, M. A. (2003) *Biochemistry 42*, 15189−15196.
16. Scarsdale, J. N., Kazanina, G., Radaev, S., Schirch, V., and Wright, H. T. (1999) *Biochemistry 38*, 8347−8358.
17. Szebenyi, D. M., Liu, X., Kriksunov, I. A., Stover, P. J., and Thiel, D. J. (2000) *Biochemistry 39*, 13313−13323.
18. Sivaraman, J., Li, Y., Larocque, R., Schrag, J. D., Cygler, M., and Matte, A. (2001) *J. Mol. Biol. 311*, 761−776.
19. Karthikeyan, S., Zhou, Q., Zhao, Z., Kao, C. L., Tao, Z., Robinson, H., Liu, H. W., and Zhang, H. (2004) *Biochemistry 43*, 13328−13339.
20. Jackson, L. K., Baldwin, J., Akella, R., Goldsmith, E. J., and Phillips, M. A. (2004) *Biochemistry 43*, 12990−12999.
21. Toney, M. D. (2001) *Biochemistry 40*, 1378−1384.
22. Brooks, H. B., and Phillips, M. A. (1997) *Biochemistry 36*, 15147−15155.
23. Johnson, K. A. (1992) *The Enzymes XX*, 1−61.
24. Stivers, J. T., Pankiewicz, K. W., and Watanabe, K. A. (1999) *Biochemistry 38*, 952−963.
25. Jackson, L. K., Brooks, H. B., Osterman, A. L., Goldsmith, E. J., and Phillips, M. A. (2000) *Biochemistry 39*, 11247−11257.
26. Patel, C. N., Adcock, R. S., Sell, K. G., and Oliveira, M. A. (2004) *Acta Crystallogr. D Biol. Crystallogr. 60*, 2396−2398.
27. Gerlt, J. A., and Babbitt, P. C. (1998) *Curr. Opin. Chem. Biol. 2*, 607−612.

BI061260H